

## J2.9 A TURBULENCE KINETIC ENERGY BUDGET ANALYSIS IN A WINDTUNNEL MODEL CANOPY

W. Yue\*, W. Zhu, C. Meneveau, M. B. Parlange, H. S. Kang, and J. Katz  
The Johns Hopkins University, Baltimore, Maryland

### ABSTRACT

Turbulent flow over a windtunnel model canopy composed of stalks is investigated by large eddy simulation (LES), and the computational results are compared with experimental data from Particle Image Velocimetry and Hotwire Anemometer measurements. There is very good agreement between the LES predictions and the experimental data. Inactive ‘sloshing’ motions are observed at the low levels of the model canopy. A detailed analysis of turbulent kinetic energy (TKE) budget indicates that the ‘sloshing’ motions are mainly driven by the pressure perturbations. Turbulence shear production is strong at the top of the stalks. The dissipation rate accounts for the largest TKE loss above the model canopy. Inside the model canopy, the work against the stalk drag is the major TKE loss. Deep inside the stalks, all the budget terms are relatively small in magnitude and the shear production nearly ceases, suggesting that the large-scale turbulent eddies are inhibited by the stalks.

### 1. INTRODUCTION

Turbulent flow over plant canopies has been an important research subject in that turbulence plays an important role since transfer of momentum, heat, water vapor, carbon dioxide, and other scalar entities between atmosphere and plants. A number of field experiments have been devoted to investigating the structures of turbulence within and above plant canopies. Turbulence in canopy flows is characterized by momentum absorption and energy dissipation by means of canopy drag throughout the whole depth of the canopy, leading to complex turbulent structures and high turbulence intermittency inside canopy. Most of the early studies were summarized and reviewed by Raupach and Thom (1981) and Finnigan (2000). A more recent windtunnel experiment using Particle Image Velocimetry (PIV) and Hotwire Anemometer (HW) techniques was performed by Zhu et al (2005), in which an array of cylindrical stalks was mounted on the bottom wall to mimic canopy plants (as shown in Fig. 1). The turbulent flow over the same windtunnel model canopy is studied using a large eddy simulation (LES) in the present paper. In the LES of a field corn plant canopy, Yue et al. (2006) used a ‘plant-scale’ approach to approximately resolve the shape of the corn plants, that predicts turbulence statistics and energy spectra in a better agreement with

the experimental data than the traditional ‘field—scale’ approach (Shaw and Schumann 1992). In the present study, the stalks are simulated in the same way as the corn plant stems. The scale-dependent Lagrangian dynamic Smagorinsky model (Bou-Zeid et al 2005) is employed in this LES. The objective of this study is first to validate the present LES by extensively comparing the LES predictions with the experimental data, and second to perform a full turbulent kinetic energy (TKE) budget analysis to provide information absent in the experimental measurements.

### 2. NUMERICAL MODELING

The filtered incompressible continuity and Navier-Stokes equations are as follows (with the spectral cut-off filter),

$$\begin{aligned} \frac{\partial \tilde{u}_i}{\partial x_i} &= 0 \\ \frac{\partial \tilde{u}_i}{\partial t} + \tilde{u}_j \left( \frac{\partial \tilde{u}_i}{\partial x_j} - \frac{\partial \tilde{u}_j}{\partial x_i} \right) &= - \frac{\partial \tilde{p}^*}{\partial x_i} - \frac{\partial \tau_{ij}}{\partial x_j} + F_i \end{aligned} \quad (1)$$

where the tilde symbol represents filtering. The modified pressure  $\tilde{p}^*$  is denoted as

$$\tilde{p}^* = \tilde{p} / \rho + \tilde{u}_k \tilde{u}_k / 2 + (\widetilde{u_m u_m} - \tilde{u}_m \tilde{u}_m) / 3 \quad (2)$$

$\tau_{ij}$  is the deviatoric part of the subgrid scale (SGS) stress,

$$\tau_{ij} = \widetilde{u_i u_j} - \tilde{u}_i \tilde{u}_j - (\widetilde{u_k u_k} - \tilde{u}_k \tilde{u}_k) \delta_{ij} / 3 \quad (3)$$

which is calculated with the scale-dependent dynamic Lagrangian model (Bou-Zeid et al 2005).  $F_i$  is the drag force per unit mass applied at the position of stalks,

$$F_i = - \frac{1}{2} C_0 \tilde{u}_{0,i} |\tilde{\mathbf{u}}_0| \frac{D}{dx dy} \quad (4)$$

where  $C_0$  is the cylinder drag coefficient, set to 1.0 in this study.  $D$  is the diameter of the corn stem.  $dx$  and  $dy$  are grid spacings in streamwise and spanwise directions, respectively.  $\tilde{u}_{0,i}$  is the upstream velocity components for the stalk, calculated at a distance of 3D upstream of the stalk points.  $|\tilde{\mathbf{u}}_0|$  is the magnitude of  $\tilde{u}_{0,i}$ .

\* Corresponding author address: Wusi Yue, The Johns Hopkins University, Department of Geography and Environmental Engineering, 3400 N. Charles Street, Baltimore, MD 21218; e-mail: [yue@jhu.edu](mailto:yue@jhu.edu)

Equations (1) are solved by applying a pseudo-spectral method in the horizontal directions and centered finite-difference method in the vertical direction (Albertson and Parlange 1999). The vertical velocity component  $w$  is staggered with horizontal components  $u$  and  $v$ . The second-order Adams-Bashforth scheme is used for time advancement. The convective terms are de-aliased by padding and truncation using the 3/2 rule (Orszag 1970).

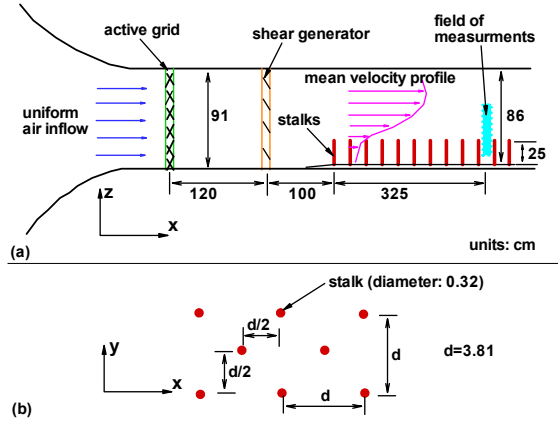


Fig. 1 Schematic of Windtunnel model canopy

### 3. RESULTS AND DISCUSSION

The predicted turbulence statistics, energy spectra, and TKE budgets by the LES are compared with the PIV and HW experimental data where available. Only two-dimensional (streamwise and vertical) data were acquired in the PIV measurement and one-dimensional (streamwise) data in the HW measurement. The superscript  $'$ , e.g., in  $-u'w'$ , denotes temporal fluctuation (deviation from the time-averaged mean value denoted as overbar). The superscript  $'$ , e.g., in  $u''$ , denotes spatial variation (deviation from the horizontally-averaged mean value denoted as  $\langle \rangle$ ). Turbulence statistics predicted by the LES is calculated in terms of temporal fluctuations. The resulting three dimensional statistics are finally averaged over the horizontal planes to describe only the overall effects of the model canopy.

Figure 2 shows the one-dimensional energy spectra of  $u''$ ,  $E_{uu}$ , from the LES, the PIV, and the HW, with respect to the streamwise wavenumber,  $k_x$ , at the four elevations from inside the stalks to above the stalks,  $z/h=0.87, 1, 1.4,$  and  $2$ . The data are normalized by the stalk height  $h$  and the friction velocity at the top of the stalks  $u_*$ . The spectra from the LES are averaged in the spanwise direction and in time. The temporal HW frequency is converted into spatial wavenumber using Taylor's Hypothesis. The energy spectra from the LES, the PIV, and the HW nearly collapse at all the four elevations. The small peaks in the LES spectra below and at the top of the stalks result from the canopy drag imposed in the numerical model. The HW spectra have the longest wavenumber span, about four decades. The LES and PIV data each span about two decades. The

energy spectra basically follow the Kolmogorov  $-5/3$  law in the inertial range at all the elevations.

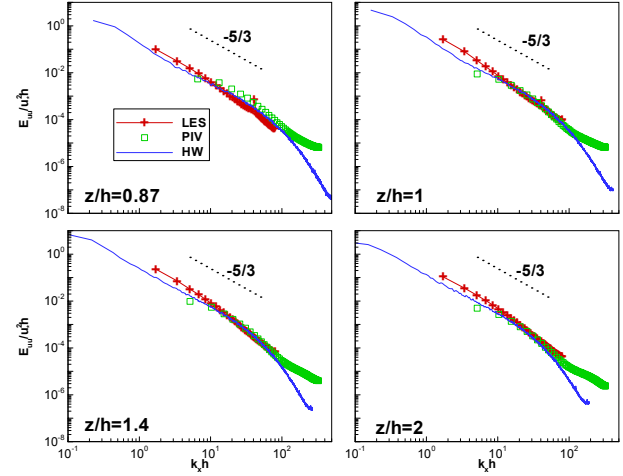


Fig.2 Energy spectra  $E_{uu}$  at four elevations

Figure 3 shows the root-mean-square (rms) velocity profiles,  $u_{rms}$ ,  $v_{rms}$ , and  $w_{rms}$ , from the LES, the PIV, and the HW, which are normalized by  $u_*$ . There is quite good agreement in  $u_{rms}$  and  $w_{rms}$  among the LES, the PIV, and the HW data. The streamwise fluctuations decrease quickly within the stalks, suggesting that the stalk drag is more efficient in extracting energy from  $u'$ . The three rms profiles from the LES show the peaks near the upper wall where the strong near-wall turbulence production occurs. The normalized  $u_{rms}$  and  $w_{rms}$  are around 1.65 and 1.15, respectively, close to the values of 1.8 and 1.2 in the corn field (Yue et al 2006). Contrast to that in the surface-layer turbulence,  $v_{rms}$  is close to  $w_{rms}$  at all levels of the windtunnel. Note that the rms from LES only contains the resolved rms, so that one expects a small under-prediction of rms from LES.

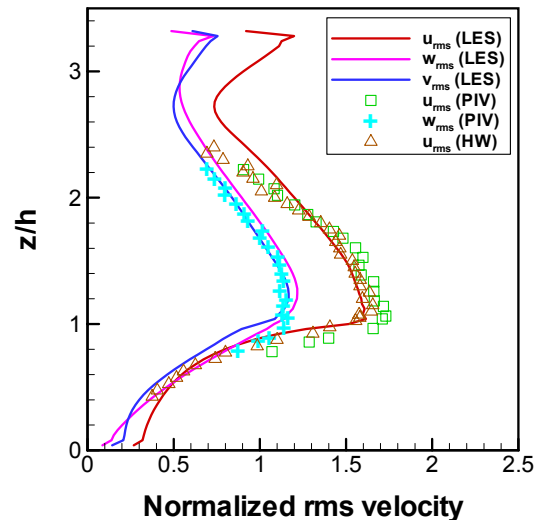


Fig. 3 RMS velocity, normalized by  $u_*$

Figure 4 shows the vertical profiles of the Reynolds shear stress,  $-\langle u'w' \rangle$ , or momentum flux, normalized by  $u_*^2$ . The agreement between the LES (which includes the mean SGS stress) and the PIV data is very good. The momentum flux decreases sharply below the top of the stalks, similar to the rms velocity in Fig. 3. In the lower layer of the model canopy, the momentum flux nearly approaches to zero, indicating that most of the momentum transported from the top of the stalks is absorbed by the upper layer of the model canopy. However, the rms velocities are finite at the same lower layer, suggesting that there exists some inactive 'sloshing' motions near the bottom (Finnigan 2000). Above the stalks, the momentum flux shows a linear profile, same as in a turbulent channel flow, suggesting that the direct effect of the model canopy to the air flow is to modulate the friction velocity at the top of the stalks. The momentum flux vanishes at  $z/h=2.7$  where the rms velocities attain their minimum values (see Fig. 3).

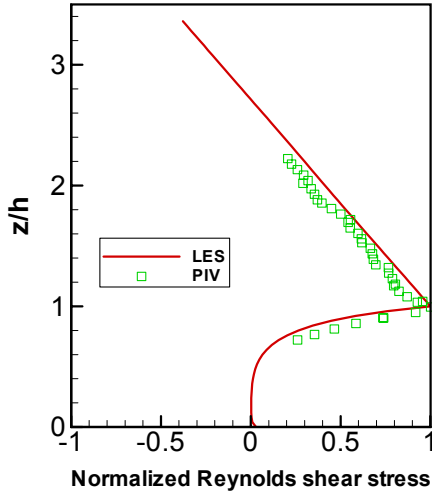


Fig. 4 Mean shear stress (sum of the resolved-scale and SGS components)

An analysis of TKE budgets can provide the information of the relative significance of various physical processes that govern turbulent motions. The resolved-scale TKE budget equation is expressed in the following equation:

$$W \frac{\partial \bar{K}}{\partial z} = \underbrace{-\overline{u'w'}}_{A_v} \frac{\partial U}{\partial z} + \underbrace{\frac{\partial \bar{K}w'}{\partial z}}_{P_s} - \underbrace{\frac{\partial \bar{p}'w'}{\partial z}}_{T_t} - \underbrace{\frac{\partial \bar{p}'w'}{\partial z}}_{T_p} - \underbrace{\frac{\partial \overline{\tau'_{iz}u'_i}}{\partial z}}_{T_{sgs}} + \underbrace{F'_i u'_i}_{W_d} + \underbrace{\overline{\tau'_{ij}S'_{ij}}}_{\epsilon_f} \quad (5)$$

The terms in Eq. (5) are referred to as  $A_v$ ,  $P_s$ ,  $T_t$ ,  $T_p$ ,  $T_{sgs}$ ,  $W_d$ , and  $\epsilon_f$ , from left to right.  $A_v$  is the vertical advection of the resolved-scale TKE by the mean flow.  $P_s$  represents the conversion of mean flow kinetic energy to the resolved-scale TKE.  $T_t$ ,  $T_p$ , and  $T_{sgs}$  represent the vertical transport of the resolved-scale TKE by

fluctuations of vertical velocity, pressure, and SGS stresses, respectively.  $W_d$  represents work against the canopy drag.  $\epsilon_f$  represents the energy transfer from the resolved-scale TKE to the SGS.

Figure 5 shows the shear production  $P_s$  and dissipation rate  $\epsilon_f$ , as a function of height. The dissipation rate  $\epsilon_f$  of the PIV data is estimated by fitting a  $-5/3$  slope line to the distribution of one-dimensional longitudinal energy spectra in the inertial range. There is excellent agreement between the LES predictions and the PIV data. The  $P_s$  profile shows a large peak at the top of the stalks where the strong wind shear occurs.  $P_s$  decreases sharply within the stalks, and nearly ceases below  $z/h=0.5$ .  $P_s$  shows another peak near the upper wall due to the large shear at the upper wall boundary layer, and approaches to zero at  $z/h=2.7$ , corresponding to the lowest turbulence intensity above the stalks. This is also the place where the Reynolds shear stress vanishes, as shown in Fig. 4.

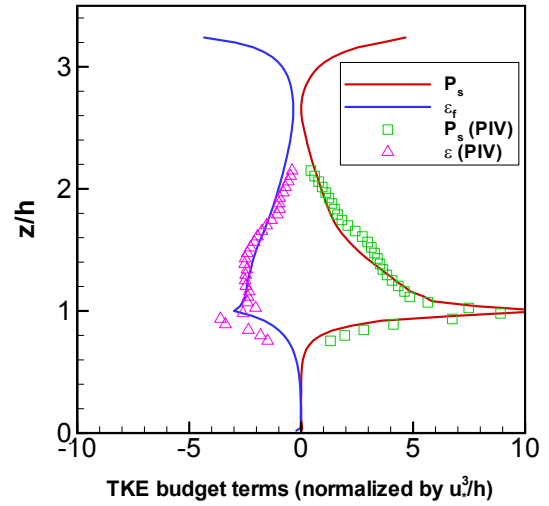


Fig. 5 TKE budget terms: shear production and dissipation

The three transport terms,  $T_t$ ,  $T_p$ , and  $T_{sgs}$  are plotted in Fig. 6. LES and the PIV profiles show that the turbulent transport  $T_t$  changes signs around the top of the stalks, indicating that the turbulent transport extracts energy from the air flow immediately above the model canopy ( $1 < z/h < 1.5$ ) and redistributes the energy into the model canopy and the upper air flow region ( $z/h > 1.5$ ). The pressure transport is of interest because a direct experimental measurement of pressure fluctuation is very difficult.  $T_p$  demonstrates a similar behavior to  $T_t$  inside and immediately above the model canopy but with smaller magnitudes. Above  $z/h=1.2$ ,  $T_p$  is opposite to  $T_t$  in sign. The pressure fluctuations extract energy from the air layer  $1 < z/h < 1.2$  and transport it into the model canopy and the upper air layer  $1.2 < z/h < 1.6$ . The SGS transport  $T_{sgs}$  is insignificant compared to  $T_t$  and  $T_p$ , except around the top of the stalks where the largest stress fluctuations occur.

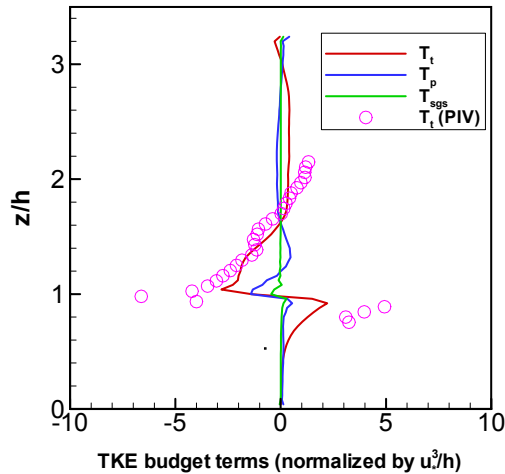


Fig. 6 TKE budget terms: turbulent transport, pressure transport, and SGS transport

Deep inside the model canopy ( $z/h < 0.4$ ), all the three transport terms are small in magnitudes.  $T_p$ , however, acts as the largest TKE supplier in this layer, as shown in Fig. 7, implying that turbulence at the lowest levels of the canopy is largely governed by pressure perturbations.  $T_t$  also appears as the other TKE supplier in this low layer of the model canopy.  $P_s$ , however, nearly vanishes due to the lower shear deep inside the model canopy. This is another indication of the aforementioned ‘sloshing’ motions at this low layer of the model canopy in that pressure perturbation is the major driving force of the flow motion there.

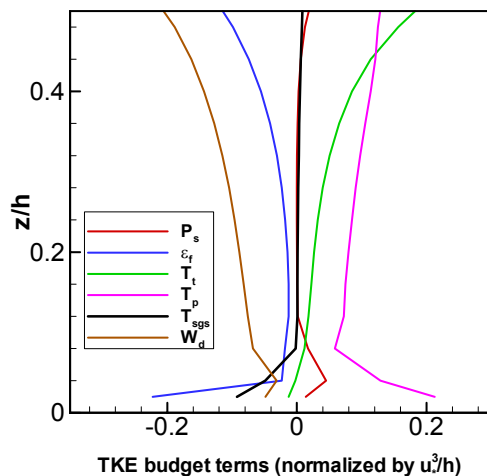


Fig. 7 TKE budget terms at low levels of the model canopy.

#### 4. CONCLUSIONS

The turbulence structure of turbulent flow over a windtunnel model canopy composed of stalks has been investigated using LES. The predictions of the LES in turbulence statistics and turbulent kinetic energy budgets are extensively compared with the PIV and HW

experimental data. Very good agreement is observed. The energy spectra predicted by the LES show a collapse with those of the PIV and the HW. The weak shear stress at the lower levels of the model canopy causes some inactive sloshing motions there: low Reynolds shear stress but finite velocity variance. These kind of sloshing motions are mainly driven by the pressure perturbations as shown from the TKE budget analysis. The shear production has a large peak at the canopy top, contributing the most of the TKE source around and above the top of the model canopy. The dissipation rate accounts for the largest TKE loss above the model canopy. Inside the model canopy, however, the work against the stalk drag is the major TKE loss. The turbulent transport and the pressure transport both appear as TKE gain inside the model canopy but loss immediately above the model canopy.

**ACKNOWLEDGMENT:** This study was supported by the National Science Foundation through Grant No. BES-0119903.

#### REFERENCE:

- Albertson, J. D., and M. B. Parlange, 1999: Surface length-scales and shear stress: implications for land-atmosphere interaction over complex terrain. *Water Resour. Res.*, **35**, 2121-2132.
- Bou-Zeid, B., C. Meneveau, and M.B. Parlange, 2005: A scale-dependent Lagrangian dynamic model for large eddy simulation of complex turbulent flows, *Phys. Fluids*, **17**, 025105.
- Finnigan, J., 2000: Turbulence in plant canopies. *Annu. Rev. Fluid Mech.*, **32**, 519-571.
- Orszag, S. S., 1970: Transform method for calculation of vector coupled sums: Application to the spectral form of vorticity equation, *J. Atmos. Sci.*, **27**, 890-895.
- Raupach, M.R., and A.S. Thom, 1981: Turbulence in and above plant canopies. *Annu. Rev. Fluid Mech.*, **13**, 97-129.
- Shaw, R.H., and U. Schumann, 1992: Large-eddy simulation of turbulent flow above and within a forest. *Boundary-Layer Meteorology*, **61**, 47-64.
- Yue, W., C. Meneveau, M.B. Parlange, W. Zhu, R. van Hout, and J. Katz 2006: Large eddy simulation study of turbulence structures within and above a corn canopy, using field- and plant-scale representations, to be submitted.
- Zhu, W., R. van Hout, L. Luznik, H.S. Kang, J. Katz, and C. Meneveau, 2005: Applying PIV for measuring turbulence just within and above a corn canopy, 6th International Symposium on Particle Image Velocimetry (CD-ROM), Pasadena, California, USA, Sept. 21-23.